



# CHORUS

This is the accepted manuscript made available via CHORUS. The article has been published as:

## Vindication of $\text{Yb}_{\{2\}}\text{Ti}_{\{2\}}\text{O}_{\{7\}}$ as a Model Exchange Quantum Spin Ice

R. Applegate, N. R. Hayre, R. R. P. Singh, T. Lin, A. G. R. Day, and M. J. P. Gingras

Phys. Rev. Lett. **109**, 097205 — Published 28 August 2012

DOI: [10.1103/PhysRevLett.109.097205](https://doi.org/10.1103/PhysRevLett.109.097205)

# Vindication of $\text{Yb}_2\text{Ti}_2\text{O}_7$ as a Model Exchange Quantum Spin Ice

R. Applegate,<sup>1</sup> N. R. Hayre,<sup>1</sup> R. R. P. Singh,<sup>1</sup> T. Lin,<sup>2</sup> A. G. R. Day,<sup>2,3</sup> and M. J. P. Gingras<sup>1,2,4</sup>

<sup>1</sup>Physics Department, University of California at Davis, Davis, CA 95616

<sup>2</sup>Department of Physics and Astronomy, University of Waterloo, Waterloo, Ontario, N2L 3G1, Canada

<sup>3</sup>Département de Physique, Université de Sherbrooke, Sherbrooke, Québec, J1L 2R1, Canada

<sup>4</sup>Canadian Institute for Advanced Research, 180 Dundas St. W., Toronto, Ontario, M5G 1Z8, Canada

(Dated: July 18, 2012)

We use numerical linked cluster (NLC) expansions to compute the specific heat,  $C(T)$ , and entropy,  $S(T)$ , of a quantum spin ice Hamiltonian for  $\text{Yb}_2\text{Ti}_2\text{O}_7$  using anisotropic exchange interactions recently determined from inelastic neutron scattering measurements and find good agreement with experimental calorimetric data. This vindicates  $\text{Yb}_2\text{Ti}_2\text{O}_7$  as a model quantum spin ice. We find that in the perturbative weak quantum regime, such a system has a ferrimagnetic ordered ground state, with two peaks in  $C(T)$ : a Schottky anomaly signalling the paramagnetic to spin ice crossover followed at lower temperature by a sharp peak accompanying a first order phase transition to the ordered state. We suggest that the two  $C(T)$  features observed in  $\text{Yb}_2\text{Ti}_2\text{O}_7$  are associated with the same physics. Spin excitations in this regime consist of weakly confined spinon-antispinon pairs. We anticipate that conventional ground state with exotic quantum dynamics will prove a prevalent characteristic of many real quantum spin ice materials.

PACS numbers: 74.70.-b, 75.10.Jm, 75.40.Gb, 75.30.Ds

The experimental search for quantum spin liquids (QSLs), magnetic systems disordered by large quantum fluctuations, has remained unabated for over twenty years [1]. One direction that is rapidly gathering momentum is the search for QSLs among materials that are close relatives to spin ice systems [2], but with additional quantum fluctuations, or *quantum spin ice* (QSI) [3, 4].

Spin ice materials, such as  $\text{R}_2\text{M}_2\text{O}_7$  ( $\text{R}=\text{Ho}, \text{Dy}$ ;  $\text{M}=\text{Ti}, \text{Sn}$ ), have magnetic rare-earth atoms ( $\text{Ho}, \text{Dy}$ ) at the vertices of a pyrochlore lattice of corner-sharing tetrahedra [2, 5]. The combination of large single ion anisotropy and exchange and dipolar interactions lead to an exponentially large number of low-energy states characterized by two spins pointing in and two spins pointing out on each tetrahedron (see Fig. 1a). This energetic constraint is equivalent to the Bernal-Fowler ice rules which endow water ice with a residual Pauling entropy per proton of  $S_P \sim (\frac{k_B}{2}) \ln(3/2)$  [6, 7]. The spin ice state, with also a residual entropy  $S_p$  [8], is not thermodynamically distinct from the paramagnetic phase. Yet, because of the ice-rules, it is a strongly correlated state of matter – a *classical* spin liquid of sorts [1, 2].

Several theoretical works have proposed that introducing quantum fluctuations to such a system, thus turning it into a QSI [3, 4], may lead to an exotic QSL phase of matter, one that possibly realizes an emergent Quantum Electrodynamics (QED) [9–11]. The search for such a phase is being vigorously pursued in many materials [3, 4]. Intense experimental [12–19] and theoretical [14–16, 19–24] interest has recently turned to  $\text{Yb}_2\text{Ti}_2\text{O}_7$  (YbTO), which has been argued to be on the verge of realizing a QSL originating from QSI physics. In fact, the combination of (i) an unexplained transition at  $T_c \sim 0.24$  K [12, 25], (ii) the controversial evidence for long-range order below  $T_c$  [26, 27] and (iii) the high sensi-

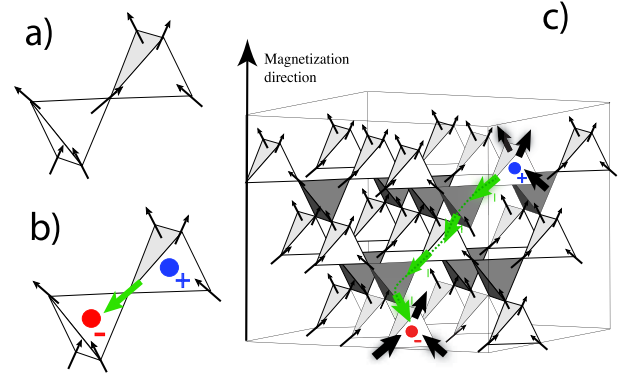


FIG. 1: (a) Two neighboring tetrahedra with spins in their two-in/two-out ground state, (b) spinon/antispinon pair, (c) spinon/antispinon pair separated by a (green) string of misaligned spins in the pyrochlore lattice.

tivity of the low-temperature ( $T < 300$  mK) behavior to sample preparation conditions [17, 18] are all tantalizing evidence that YbTO has a fragile and perhaps unconventional ground state. Thus, explaining YbTO is a key milestone in the study of QSI in a real materials context.

The possibility that a QED-like framework [9, 10] may be relevant to describe the physics of the QSI class of materials [23, 28] is exciting as it could lead to the first unequivocal identification of a QSL with its accompanying emergent deconfined excitations and gauge boson. Unfortunately, a quantitative theoretical bridge between experiments and QED-like theory, capable of dealing with thermodynamic properties of realistic QSI models, is currently lacking. This is where our work, which employs the numerical-linked cluster (NLC) method, comes in [29, 30]. Highly frustrated magnetic quantum systems

are not amenable to large-scale quantum Monte Carlo simulations because of the so-called sign problem. While the density matrix renormalization-group (DMRG) is a powerful method for 1-dimensional systems, and exact diagonalization has proved useful in two-dimensions, these methods are much less useful in three-dimensions. Using YbTO as a benchmark, we show below that NLC allows for a reliable and accurate calculation of thermodynamic properties of such systems as a function of temperature in the regime of short-range correlations and over a range of parameters.

Anisotropic exchange interactions,  $\{J_e\}$ , are expected to drive exotic quantum physics, including QSI, in pyrochlore oxides [3, 4, 16, 23, 28]. While these have been argued to be at play in YbTO for some time [14], there is at present no consensus as per their values [14–16, 19–21], an issue that stands in the way of making progress in understanding this system. By calculating the specific heat,  $C(T)$ , in a reliable manner using NLC expansions, we show that the  $\{J_e\}$  values of Ross *et al.* [16] provide excellent agreement with experiments, hence validating their exchange parameters over others [14, 15, 19, 20].

We also find an excellent agreement between the theoretical entropy,  $S(T)$ , calculated for YbTO parameters, by going down in  $T$  starting from a value of  $k_B \ln 2$  at  $T = \infty$ , and the experimental entropy obtained by assuming zero entropy at  $T = 0$  and integrating the  $C(T)/T$  data through the sharp peak around 0.24 K. This agreement does suggest that the experimentally observed sharp peak in YbTO may be consistent with the model. However, since our numerical results are valid only at relatively high  $T$ , we can not rule out the possibility that the model may have an entropy that would only decrease gradually to zero as  $T$  goes to zero without displaying a transition. Such a second peak, and the development of long-range order, is also found in our Monte Carlo simulations of a pertinent effective classical model.

Finally, we use perturbative arguments to show that despite a conventional ground state, the spin excitations consist of spinon/antispinon pairs connected by (Dirac-like [31, 32]) strings of reversed spins, whose confinement length  $l_s$  diverges in the limit of small quantum exchanges. We propose that these excitations should ultimately form the basis for describing what we expect to be highly unconventional inelastic neutron spectra [24].

*Model & Method* – The anisotropic exchange QSI model is defined by the nearest-neighbor Hamiltonian [16, 23] on the pyrochlore lattice

$$\begin{aligned} H_{\text{QSI}} = & \sum_{\langle i,j \rangle} \{ J_{zz} S_i^z S_j^z - \lambda J_{\pm} (S_i^+ S_j^- + S_i^- S_j^+) \\ & + \lambda J_{\pm\pm} [\gamma_{ij} S_i^+ S_j^+ + \gamma_{ij}^* S_i^- S_j^-] \\ & + \lambda J_{z\pm} [S_i^z (\zeta_{ij} S_j^+ + \zeta_{ij}^* S_j^-) + i \leftrightarrow j] \}. \quad (1) \end{aligned}$$

$\gamma_{ij}$  is a  $4 \times 4$  complex unimodular matrix, and  $\zeta = -\gamma^*$  [16]. The  $\hat{z}$  quantization axis is along the local [111] direc-

tion, and  $\pm$  refers to the two orthogonal local directions. We take  $\lambda = 1$ , except when stated otherwise.

Recently Ross *et al.* [16] used inelastic neutron scattering data in high magnetic field to deduce the  $\{J_e\}$  exchange parameters for YbTO:  $J_{zz} = 0.166 \pm 0.04$ ,  $J_{\pm} = 0.05 \pm 0.01$ ,  $J_{\pm\pm} = 0.05 \pm 0.01$ , and  $J_{z\pm} = -0.14 \pm 0.01$ , all in meV. These parameters have also been determined through an analysis of the zero-field energy-integrated paramagnetic neutron scattering [15, 19], but the values of the  $\{J_e\}$  parameters disagree significantly – an issue that we address in the Supplementary Material [33].

We calculate the thermodynamic properties of the model (1) using an NLC expansion that includes all contributions from clusters upto four tetrahedra [29, 30, 33]. Such an expansion is numerically exact in two limits. It is so at high temperature because the contributions from larger clusters neglected here are  $O(\beta^6)$ , where  $\beta \equiv 1/T$ . It is also exact at high-field  $h$  at all temperatures, because corrections are  $O((J/h)^5)$  at  $T = 0$ , with further exponentially small corrections  $\exp(-ch/T)$  at  $T \neq 0$ . The only region where it is not necessarily accurate is when both  $T$  and  $h$  are small. A tetrahedron-based NLC is particularly suited to spin ice related systems. Indeed, it was recently shown that for classical spin ice models, just first order NLC is equivalent to the Pauling approximation [6] and gives  $C(T)$  and  $S(T)$  for all  $T$  within a few percent accuracy [34]. Euler extrapolations [35] are used to further improve the convergence of the calculations at low  $T$ . Details on the NLC expansions can be found in the Supplementary Material [33].

Figure 2 shows  $C(T)$  calculated with different NLC orders. By 4<sup>th</sup> order, there is good convergence to temperatures below the  $C(T)$  peak at  $\sim 2$  K. Applying Euler transformations [35] improves the convergence down to slightly below 1 K. The experimental data from Refs. [25], shown for comparison, agree well with the NLC results. This agreement shows that the  $\{J_e\}$  parameters are not substantially changed compared to the high-field ( $h = 5$  Tesla) values [16]. Using the  $\{J_e\}$  of Refs. [15, 19] gives substantially different  $C(T)$  results [33].

Figure 3 shows  $S(T)$  calculated by NLC, together with the entropy obtained by integrating the experimental  $C(T)/T$  data of Ref. [25], which we found ideally suited to perform a comparison with NLC [33]. The entropy converges to lower temperature slightly better than  $C(T)$  where, with Euler transformations,  $S(T)$  converges down to about 0.7 K, matching well with the experimental entropy values over the overlapping temperature range. Note that the agreement of the NLC  $S(T)$  with the experimental  $S(T)$  is *not* redundant with the agreement found above for  $C(T)$  (since  $S(T_2) - S(T_1) = \int_{T_1}^{T_2} [\frac{C(T)}{T}] dt$ ). The experimental  $S(T)$  was obtained assuming a zero residual entropy at  $T_1 \lesssim 100$  mK ( $S^{\text{exp}}(T_1) = 0$ ) while the NLC  $S(T)$  was obtained taking the paramagnetic entropy  $S^{\text{NLC}}(T_2 \rightarrow \infty)$  to be  $k_B \ln(2)$ . Hence, there is no a pri-

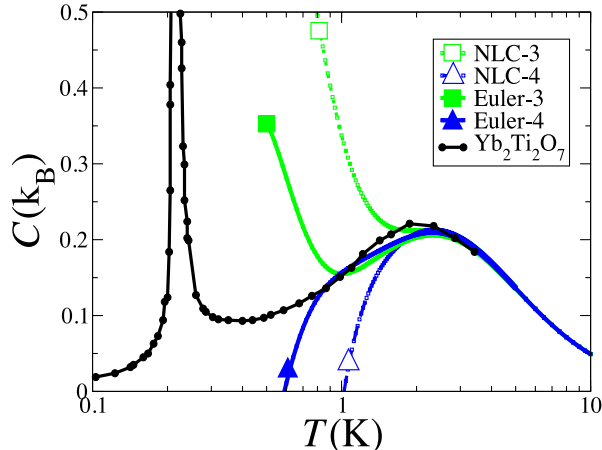


FIG. 2: Heat capacity,  $C(T)$ , per mole of Yb for the model parameters in Ref. [16], in units of the Boltzmann constant  $k_B$ , calculated via NLC (up to 4<sup>th</sup> order NLC together with Euler extrapolations) are compared with experimental data for  $\text{Yb}_2\text{Ti}_2\text{O}_7$ . The black circles are data from Ref. [25].

ori reason why the two entropies should mesh so well with each other in the 0.7 K – 4 K temperature range where strong correlations develop [15, 16]. Thus, the observed  $S(T)$  agreement between experiment and NLC, along with that for  $C(T)$  in Fig. 2, provides compelling evidence that we have at hand with Eq. (1) a quantitative model of YbTO, which may also explain the phase transition around 0.24 K. This is the main result of this paper.

*Perturbative considerations* – We now turn to the perturbative regime  $\lambda \ll 1$  in Eq. 1 [16, 23]. To second order in  $\lambda$ , only  $J_{z\pm}$ , by far the largest quantum term for YbTO, leads to a degeneracy-lifting classical potential for different spin-ice configurations. It amounts to a fluctuation-induced ferromagnetic exchange coupling  $J_3 \equiv -3\lambda^2 J_{z\pm}^2 / J_{zz}$  [23] between shortest distance spins on the same tetrahedral sublattice that share a neighbor [36]. It leads to the selection of a  $\mathbf{q} = 0$  long-range ordered ground state in which all tetrahedra have the same spin configuration making a net magnetic moment along one of the  $\langle 100 \rangle$  cubic directions. To calculate  $C(T)$  and  $S(T)$  in the perturbative regime at low  $T$ , we turn to classical loop Monte Carlo simulations [37] of the  $J_{zz} - J_3$  model [33]. These reveal a very sharp lower temperature  $C(T)$  peak accompanying a first order phase transition to the aforementioned  $\mathbf{q} = 0$  state (see Fig. S5 [33]).

*Excited states in the perturbative regime: spinons and strings* – A surprise of the perturbative treatment is that, while the ground state is classical, the spin-flip excitations remain non-trivial and of quantum nature. This is because, once a spin is flipped in a spin-ice state, creating

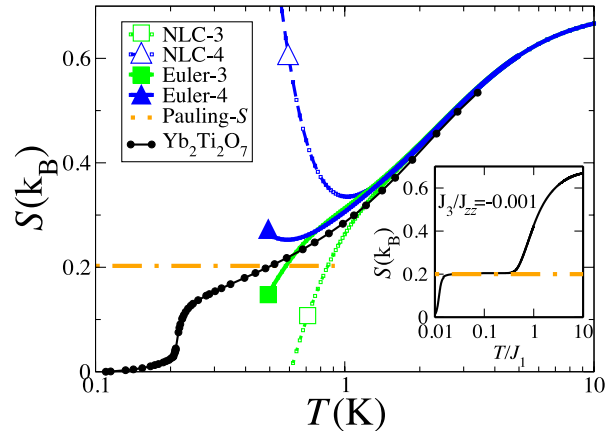


FIG. 3: Entropy,  $S(T)$ , per mole of Yb, in units  $k_B$  following the methods described in the caption of Fig. 2. The black circles are obtained by integrating the data from Ref. [25] excluding the nuclear (hyperfine) contribution. The Pauling entropy  $S_P \sim \frac{k_B}{2} \ln \frac{3}{2}$  is shown as a horizontal line. The inset shows  $S(T)$  in the perturbative regime with  $J_3/J_{zz} = -0.001$ . A clear plateau at  $S(T) \approx S_P$  is seen, followed at lower  $T$  by a precipitous drop of  $S(T)$  (i.e. latent heat) accompanying the transition to long range FM order [33].

a spinon/antispinon pair [32], the pair can hop through  $J_{z\pm}$  acting through *first order* degenerate perturbation theory. Thus, the dispersion bandwidth in the excited state manifold is  $O(\lambda J_{z\pm})$ , *much larger* than the dispersion within the low-energy manifold of spin ice states, which is only  $O(\lambda^2 J_{z\pm}^2 / J_{zz})$ .

A sketch of a spinon/antispinon pair is shown in Figs. 1b and 1c. Note that only spins inside the tetrahedron “already” containing spinons are flippable in first order degenerate perturbation theory. Hence, the connecting string of misaligned spins can only fluctuate by higher order processes involving closed loops with alternating in-out spins [24]. Thus the renormalized string tension per unit length remains finite and of order  $J_3$ . One can estimate the typical string length as the length,  $l_s$ , at which the cost of the string becomes comparable to the delocalization energy of the spinon/antispinon pair. The string energy per unit length goes as  $\sim J_3 \sim \lambda^2 J_{z\pm}^2 / J_{zz}$ , whereas the delocalization energy (spinon bandwidth) goes as  $\lambda J_{z\pm} / J_{zz}$ . This gives  $l_s$  scaling as  $(1/\lambda)(J_{zz}/J_{z\pm})$ , which diverges as  $(\lambda J_{z\pm}) \rightarrow 0$ . The spinon/antispinon, with accompanying strings, are a description of the excitations most useful in the limit of small  $\lambda$ . As one moves farther from the  $J_{\pm} = J_{\pm\pm} = J_{z\pm} = 0$  classical spin ice and into the ferrimagnetic regime, a conventional magnon description may become more adequate. In the intermediate regime, either description would require consideration of strong scattering of their

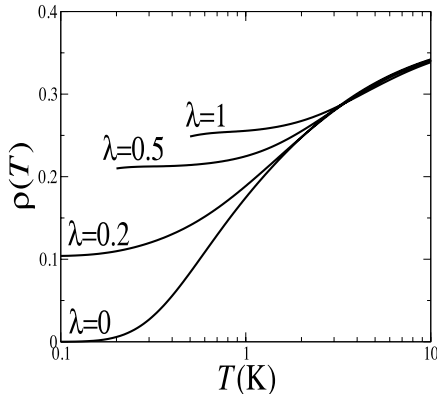


FIG. 4: Defect density,  $\rho(T)$ , calculated using NLC, shown down to a temperature where 3rd and 4th order Euler transforms agree. Here, quantum exchanges are scaled with respect to the YbTO  $\{J_e\}$  parameters by different values of  $\lambda$ .

quasi-particles (spinons or magnons).

A detailed theory of neutron scattering in this ferrimagnetic phase is not attempted here, but we anticipate it to follow the proposal of Ref. [24]. At temperatures above the transition to the  $\mathbf{q} = 0$  long-range ordered state, the system explores the classical two-in/two-out spin ice states and should display singularities (pinch points, PPs) in neutron scattering [38] rounded off by the finite density of thermally excited spinon/antispinon defects [32, 38]. While the system has thermally smeared PPs above the ferrimagnetic transition and no static PPs well below the transition, it may display some remnant of PPs in the spin dynamics at higher energies [39] These interesting issues deserve further attention. We note in passing that very recent work explores the neutron scattering properties of a minimal QSI model [39].

*Beyond the  $\lambda \ll 1$  regime* – Why is the transition temperature of YbTO so low? As discussed by Ross *et al.* [16], the low  $T$  peak in  $C(T)$  is at a temperature lower than mean-field theory by an order of magnitude. Comparing  $C(T)$  for the quantum model with different  $\lambda$  with the corresponding classical model with the perturbative  $J_3/J_{zz}$  value provides a hint of the reason why [33]. It shows that in the classical  $J_{zz} - J_3$  model the long-range order moves steadily up with increasing  $J_3$ , even beyond the short-range order  $C(T)$  peak. In contrast, the quantum systems with different  $\lambda$  continue to display a short-range order  $C(T)$  peak and presumably long-range order only occurs at a much lower  $T$ .

Another reason for a reduced  $T_c$  comes from considering the temperature dependence of the defect (spinon/antispinon) density [32],  $\rho(T)$ , as calculated by NLC (see Fig. 4 and Figs. S3 and S4 [33]). To illustrate the point, we show  $\rho(T)$  for several different  $\lambda$  val-

ues. Convergence increases to lower  $T$ , with decreasing  $\lambda$ , as expected. One finds that as  $T$  drops below the hump in  $C(T)$ ,  $\rho(T)$  displays a plateau-like region, whose value increases steadily with increasing  $\lambda$ . This indicates that the states *within* the spin-ice manifold develop large spinon/antispinon spectral weight, thus strongly renormalizing all low energy scales and, presumably, leading to a reduced  $T_c$ .

*Discussion: What constitutes an exchange QSI?* – We suggest that a double-peaked  $C(T)$  with an entropy between the peaks comparable to  $S_P$  is the hallmark of an exchange quantum spin ice (QSI). However, one is unlikely to find an exact plateau at  $S(T) \approx S_P$  outside the perturbative (small  $\lambda$ ) regime (see Fig. 3) [33]. Evidence for such a double-peaked structure and quasi-separation of the energy/temperature scales associated with short and long-range physics has also been sought in other systems where quantum spin liquid physics may exist [40].

According to the gauge mean-field theory of Ref. [23], at low temperature below which short-range spin ice correlations develop, a system may exhibit either conventional ferrimagnetic (FM) order, a Coulombic ferromagnet (CFM) or a full-blown quantum spin-liquid (QSL), depending on its exchange parameters. The largest quantum exchange term in YbTO is  $J_{z\pm}$ , which favors the FM state and which we believe is the origin of the 0.24 K transition in the best samples [17, 18, 26]. It remains to be seen if there exist materials for which  $J_{\pm}$ , that favors the QSL [9, 10, 23], is the dominant quantum term. Since  $J_{z\pm}$  is zero for non-Kramers ions (e.g. Pr, Tb) [28], and virtual crystal field excitations [3] in Tb-based pyrochlores are a fundamentally different pathway from anisotropic superexchange [4] to generate anisotropic  $\{J_e\}$  couplings between effective spins 1/2 [3, 4], the prospect to eventually find a QSI-based QSL among rare-earth pyrochlores [5] is perhaps promising.

Having demonstrated through NLC expansions that the anisotropic exchange model of Eq. (1) with the  $\{J_e\}$  values of Ref. [16] describes quantitatively  $\text{Yb}_2\text{Ti}_2\text{O}_7$ , we anticipate that NLC will also be useful to successfully describe other magnetic pyrochlore oxides and other highly-frustrated three-dimensional magnetic systems for which there are essentially no other reliable unbiased quantitative methods available.

This work is supported in part by NSF grant number DMR-1004231, the NSERC of Canada and the Canada Research Chair program (M.G., Tier 1). We acknowledge very useful discussions with P. Holdsworth, B. Javanparast, K. Ross and J. Thompson. We thank P. Dalmas de Réotier for providing the specific heat data of Ref. [17].

---

[1] L. Balents, Nature **464**, 199 (2010).

- [2] M. J. P. Gingras, in *Introduction to Frustrated Magnetism*, (Springer, 2011) arXiv:0903.2772 .
- [3] H. R. Molavian *et al.*, Phys. Rev. Lett. **98**, 157204 (2007).
- [4] S. Onoda and Y. Tanaka, Phys. Rev. Lett. **105**, 047201 (2010).
- [5] J. S. Gardner *et al.*, Rev. Mod. Phys. **82**, 53 (2010).
- [6] L. Pauling, J. Am. Chem. Soc. **57**, 2680 (1935).
- [7] W. F. Giaquie and J. W. Stout, J. Am. Chem. Soc. **58**, 1144 (1936).
- [8] A. P. Ramirez *et al.*, Nature **399**, 333 (1999); A. L. Cornelius and J. S. Gardner, Phys. Rev. B **64**, 060406 (2001).
- [9] M. Hermele *et al.*, Phys. Rev. B **69**, 064404 (2004).
- [10] A. H. Castro Neto *et al.*, Phys. Rev. B **74**, 024302 (2006).
- [11] A. Banerjee *et al.*, Phys. Rev. Lett. **100**, 047208 (2008); N. Shannon *et al.*, *ibid* **108**, 067204 (2012).
- [12] J. A. Hodges *et al.*, Phys. Rev. Lett. **88**, 077204 (2002).
- [13] K. A. Ross *et al.*, Phys. Rev. Lett. **103**, 227202 (2009).
- [14] H. B. Cao *et al.*, J. Phys. Condens. Matter **21**, 492202 (2009).
- [15] J. D. Thompson *et al.*, Phys. Rev. Lett. **106**, 187202 (2011).
- [16] K. A. Ross *et al.*, Phys. Rev. X **1**, 021002 (2011).
- [17] A. Yaouanc *et al.*, Phys. Rev. B **84**, 172408 (2011).
- [18] K. A. Ross *et al.*, Phys. Rev. B **84**, 174442 (2011).
- [19] L.-J. Chang *et al.*, arXiv:1111.5406
- [20] B. Z. Malkin *et al.*, J. Phys. Cond. Matter **22**, 276003 (2010).
- [21] S. Onoda, J. Phys.: Conf. Series., **320**, 012065 (2011).
- [22] J. D. Thompson *et al.*, J. Phys. Condens. Matter **23**, 164219 (2011).
- [23] L. Savary and L. Balents, Phys. Rev. Lett. **108**, 037202 (2012)
- [24] Y. Wan and O. Tchernyshyov, arXiv:1201.5314
- [25] H. W. J. Blöte *et al.*, Physica **43**, 549 (1969).
- [26] Y. Yasui *et al.*, J. Phys. Soc. Jpn. **72**, 3014 (2003).
- [27] J. S. Gardner *et al.*, Phys. Rev. B **70**, 180404(R) (2004).
- [28] SunBin Lee *et al.*, arXiv:1204.2262.
- [29] J. Oitmaa, C. Hamer and W. Zheng, *Series Expansion Methods for strongly interacting lattice models* (Cambridge University Press, 2006).
- [30] M. Rigol *et al.*, Phys. Rev. Lett. **97**, 187202 (2006); Phys. Rev. E **75**, 061118 (2007); Phys. Rev. E **75**, 061119 (2007).
- [31] C. Castelnovo *et al.*, Nature **451**, 42 (2008).
- [32] To relate our presentation more directly to the compact lattice QED context set in Refs. [9, 10], in which confinement in three-dimensions is traditionally referred to the strong (electric charge) coupling, we refrain from using the language of “monopoles” employed in Ref. [31] to label local defects in the ice rule of the parent classical spin ice. We use instead the more traditional wording of spinon/antispinon to label finite energy excitations out of the 2in/2out spin ice manifold.
- [33] See Supplementary Material.
- [34] R. R. P. Singh and J. Oitmaa, Phys. Rev. B **85**, 144414 (2012).
- [35] See for example, *Numerical Recipes*, by W. H. Press *et al*, Cambridge University Press (1989), Page 133.
- [36] These are geometrically 3rd neighbors on the pyrochlore lattice but not all 3rd neighbors belong to this category.
- [37] R. G. Melko and M. J. P. Gingras, J. Phys.: Condens. Matter **16**, R1277 (2004).
- [38] C. L. Henley, Annu. Rev. Cond. Matt. Phys. **1**, 179 (2010).
- [39] O. Benton *et al.*, arXiv:1204.1325.
- [40] V. Elser, Phys. Rev. Lett. **62**, 2405 (1989). N. Elstner and A. P. Young, Phys. Rev. B **50**, 6871 (1994).